International Journal of Thermophysics, Vol. 11, No. 4, 1990

Picosecond Laser Heating and Melting of Graphite[1]

A. M. Malvezzi[2]

Ultrashort laser pulses impinging onto solid, strongly absorbing surface deposit their energy within an absorption depth from the surface. This localized energy deposition may result in rapid and very efficient heating of the surface to temperatures far exceeding the melting or boiling point. Temperature evolution at the surface of samples and their electronic structure may be studied with nonperturbing, time-resolved optical diagnostic techniques. Picosecond laser pulses provide the fastest means for heating matter at high temperature, since the characteristic energy transfer times from photoexcited electrons to the lattice occur in this time scale. Surface evaporation is not affecting the observations in this time scale, simply because there is no time for the surface atoms to escape. As an illustration, measurements on graphite are presented here. The complex index of refraction of highly oriented pyrolytic graphite (HOPG) during picosecond laser irradiation has been measured at 1.06 μm via time-resolved ellipsometry at angles of incidence up to 80°. In particular, a value of the complex index of refraction for the liquid phase has been derived.

KEY WORDS: carbon; ellipsometry; graphite; laser heating; phase transition; optical measurements; ultrafast optical techniques.

1. INTRODUCTION

Optical properties of heated matter may provide information on thermophysical parameters of relevance in science and technology. In particular, the dependence on temperature and wavelength of the optical quantities being measured may be crucial in retrieving the relevant electronic structure of high temperature solid and liquid phases. The intrinsically nonperturbing characteristics of optical probes compare favorably with other methods. The use of coherent, high-power laser radiation as a heating

[1] Paper presented at the First Workshop on Subsecond Thermophysics, June 20–21, 1988, Gaithersburg, Maryland, U.S.A.

[2] Dipartimento di Elettronica, Universitá di Pavia, Via Abbiategrasso 209, I27100 Pavia, Italy.

0195-928X/90/0700-0797$06.00/0

source for thermophysical experiments adds several advantages to optical diagnostic techniques. First, energy is delivered to the sample in a localized way, so that highly efficient heating may result and small specimens may be used. Second, use of *ultrashort* laser pulses results in very fast heating of absorbing materials near the illuminated surface. Since in this case the thickness of the heated layer is determined by the optical absorption coefficient rather than the thermal diffusion length inside the material, extremely high temperatures may be achieved near the surface of the sample. Third, the evaporation of material from the heated surface, which may affect the optical properties of the surface itself, is minimized because (a) very little energy is given to the material so that samples remain hot for very short times and (b) there is not time enough for the atoms to escape from the surface during the laser interaction.

In this paper, some general features of the interaction of pulsed laser beams with condensed samples are presented and discussed. The relevant optical diagnostic techniques for ultrashort laser pulses are briefly discussed. As an example, heating of graphite by picosecond laser pulses is considered in a series of measurements of time-resolved reflectivity. The results of time-resolved ellipsometry on the same material are also briefly discussed.

2. PRINCIPLES OF LASER HEATING

The interaction of visible photons with matter proceeds via electronic excitation. In metals, electrons are excited by the radiation via free–free transitions. In semiconductors, interband transitions occur when the photon energy $h\nu$ exceeds the band gap energy E_g. A plasma of electrons and holes in the solid can be generated when $h\nu < E_g$ by multiphoton absorption. When a sufficient density of carriers is accumulated, interband and free carrier absorption becomes operative and the interaction proceeds as in metals. At very high laser intensities, multiphoton absorption can directly ionize the surface. In this case, a plasma in front of the solid surface is generated which absorbs light and promotes further ionization on the surface.

The transfer of energy from the hot electrons toward the lattice occurs well within the picosecond time scale via phonon emission. Thus, in strongly absorbing materials, steep temperature gradients are generated and the heat diffuses inside the bulk with a diffusion coefficient $D_{th} = k/c_v$, where k is the thermal conductivity and c_v the specific heat per unit volume of the material. With nanosecond laser pulses of duration t_p the diffusion length $(D_{th} t_p)^{1/2}$ is, for most absorbing materials, much longer than the absorption length $1/\alpha$. Thermal gradients are thus smoothed by heat diffu-

sion into the bulk. This is not the case with picosecond heating laser pulses, where $(D_{\text{th}} t_{\text{p}})^{1/2} < 1/\alpha$ holds in most cases. A one-dimensional approximate description of this situation yields the following result for the temperature increase $T - T_0$ at the surface of the laser-heated sample at the end of the heating pulse:

$$c_{\text{v}}(T - T_0) \approx (1 - R)\alpha \int_0^{t_{\text{p}}} I \, dt \tag{1}$$

where I is the intensity profile of the laser pulse ($\text{W} \cdot \text{cm}^{-2}$) and R is the reflectivity of the surface, assumed here independent from the temperature. The above expression is to be compared with the analogous one deduced for diffusion-dominated heating processes, typical of nanosecond laser pulse heating:

$$c_{\text{v}}(T - T_0) \approx \frac{(1 - R)}{\sqrt{D_{\text{th}} t_0}} \int_0^{t_{\text{p}}} I \, dt \tag{2}$$

Thus, for the same temperature rise, the laser energy in this case has to be increased by a factor of $\alpha(D_{\text{th}} t_{\text{p}})^{1/2} \gg 1$.

When the surface is heated above the melting point, evaporation *during* the picosecond laser pulse duration is likely to be negligible [1]. The recession of a hot surface due to evaporation at a temperature T during the laser pulse duration t_{p} is given by $d_{\text{evap}} = (\rho_{\text{g}}/\rho_{\text{s}})\, v_{\text{th}} t_{\text{p}}$, $v_{\text{th}} \approx (kT/m)^{1/2}$ being the component of the average thermal velocity of the evaporating particles normal to the surface and ρ_{g} and ρ_{s} the densities of the gas and solid phase, respectively. For a surface temperature of ≈ 5000 K, even with a density ratio $(\rho_{\text{g}}/\rho_{\text{s}}) = 0.01$, the amount of evaporated solid matter amounts to a fraction of a monolayer in the picosecond regime. Also, due to the smaller amount of energy deposited, the total evaporated material for a given maximum temperature at the surface is much smaller than the amount evaporated in a nanosecond laser pulse. These unique properties of the picosecond irradiation regime are extremely attractive for investigation of the high-temperature (0.5- to 1-eV) properties of matter, since both thermal diffusion and evaporation are simultaneously minimized for a suitable time interval. Surfaces at very high temperatures are obtained and may be studied before serious evaporation sets in.

Heating of condensed matter via laser pulses in the femtosecond regime results in different temperatures associated with electrons and lattice, since the characteristic energy transfer time of the order of 1 ps. The higher rate of energy deposition may increase the electron temperature much above the lattice temperature during the laser pulse. Equal values

for the temperatures will be reached at the rate of energy transfer from electrons to phonons. Moreover, other high-energy electron effects seem to distribute the laser pulse energy over distances much in excess of the absorption length [2], thus decreasing the overall efficiency of the process. Therefore, reduction of laser pulse duration below 1 ps does not result in more efficient *lattice* heating of condensed matter. However, since the threshold laser intensity for plasma formation in front of a solid target increases with decreasing laser pulse duration, some experimental advantages may be expected in the study of the extreme temperatures reached by condensed matter.

The properties of the hot surfaces created in this way may be studied with the use of *in situ* optical techniques. Basically, information on thermophysical parameters may be derived from evaluation of reflectivity and/or transmission versus wavelength for different excitation conditions. Through such measurements, as explained below, information on the optical dielectric function of the material at the conditions of the experiment may be obtained. Evaluation of these parameters critically depends on the excitation of the surface. Unwanted effects due for instance to the spatial disuniformity created below the surface have to be carefully taken into account.

3. EXPERIMENTAL TECHNIQUES

The experimental setup for performing picosecond laser heating measurements is centered around a pulsed picosecond laser source which simultaneously provides the energetic pulse for heating the material as well as the temporal resolution necessary for transient optical measurements. The Nd:YAG mode-locked laser has proved to be an ideal source for such measurements. The output radiation (at $\lambda = 1.06\ \mu m$), emitted in ≈ 30-ps pulses of a few millijoules in total energy, may be frequency converted via harmonic generation in nonlinear crystals, thus reaching visible and ultraviolet wavelengths with fair conversion efficiency. Also, the use of Raman shifting liquids or high-pressure gases allows one to obtain infrared coherent pulses. By the same techniques a finer tuning of the wavelength in the visible may be obtained.

The pump and probe optical technique, illustrated schematically in Fig. 1, has been extensively used for this kind of measurements. The laser pulse is focused on the surface of the sample and provides the excitation. A small fraction of it is extracted from the main beam, eventually frequency converted and time delayed by passing it through a variable optical delay line. This probing beam is then focused in the center of the heated area of

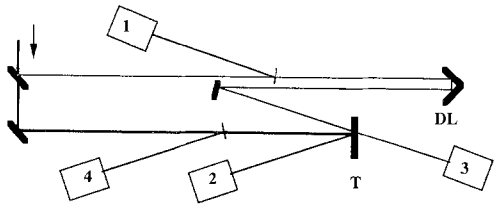

Fig. 1. Schematic diagram of a pump and probe experiment. T, target; DL, delay line; 1 to 4, optical detectors.

the sample, and the reflected and/or transmitted beam energies are measured by light detectors. These signals, once normalized, provide reflectivity and/or transmission values for the probe wavelength *at the relative time* determined by the delay line setting. It is important to note that, here, the temporal resolution is determined by the duration of the probing pulse and not by the response of the detectors. The probe beam is, in general, focused in the center of the heated area of the sample by the pump beam in order to avoid spatial averaging effects across the excited area of the sample. This relative positionning of the beams and their good spatial quality are necessary for a precise calibration of the laser fluence and provide quasi-one-dimensional geometry for the experiment when the ratio of the pump-to-probe spot radii is large.

From the instantaneous values of reflectivity and transmission one can, in principle, deduce the corresponding temporal evolution of the complex index of refraction n of the material during the interaction. In particular, characteristic changes of the optical properties above specific threshold values for the laser excitation indicate the onset of a transformation on the surface of the sample such as a phase transition to a liquid state. This technique has been extensively used in studies of the interaction of laser pulses with semiconductor surfaces [3]. The optical response at different probing wavelengths reveals distinctive differences due to different sensitivities to lattice or carrier contributions in the optical dielectric function. In particular, long-wavelength radiation is more sensitive to variations in the free carrier density, and it becomes less important at short wavelengths.

When, as is frequently the case, the material under study is optically thick, transmission measurements are precluded and the above-mentioned technique does not provide sufficient information for the evaluation of n. An alternative possibility is, however, given by transient ellipsometric measurements. This approach has already been used in transient situations for the determination of the optical constants of molten silicon under

nanosecond [4] and picosecond [5] irradition. By using polarized probe radiation impinging onto the sample at an angle of incidence ϑ, the reflectivities R_p and R_s for radiation polarized in (p) and perpendicularly to (s) the plane of incidence may be evaluated. Using Fresnel formulae, which express these quantities in terms of ϑ and the complex index of refraction n, its real (n) and imaginary (k) parts may be estimated during the interaction. At small angles of incidence, the determination of the complex index of refraction n is extremely sensitive to uncertainties in the determination of $R_{s,p}$. On the other hand, when ϑ is large, and more experimental uncertainties are present, n is less affected by the uncertainties on $R_{s,p}$.

Once n has been determined for a given excitation, the structural properties of the excited material may be deduced from the values of the dielectric function $\varepsilon = \varepsilon_1 + i\varepsilon_2 = n^2$ obtained at different wavelengths and a model for lattice and plasma contributions to ε. This is particularly true when studying phase transformations in which both contributions may vary considerably.

4. TRANSIENT OPTICAL PROPERTIES OF PHOTOEXCITED GRAPHITE

The techniques illustrated above have been used in several experiments caried on samples of highly oriented pyrolytic graphite (HOPG). Graphite is known to melt at very high temperature and high pressure (≈ 100 atm). Experimental evidence of melting at ambient pressure [6] has been claimed. However, its properties at and above the melting point are far from being well established. The use of short optical pulses of low energy and high intensity seems must suited for investigating this material.

Postmortem analysis of nanosecond laser-irradiated samples have revealed that surface melting has occurred during the laser pulse [7]. With such pulses, however, direct observation of the surface was impeded by the optical opacity of the material ejected from the hot, liquid surface. Picosecond pump and probe experiments, on the other hand, were able to monitor the temporal evolution of the reflectivity of the surface *during* the heating phase. Optical absorption of the probe beam at laser fluences much higher than the ones required to melt the surface was negligible, as expected. On the other hand, detailed studies of picosecond irradiated samples using Raman techniques revealed substantially the same disordered microstructure as the one found in nanosecond samples, indicating that the same transformations occur in the two cases [8]. Both classes of experiments, therefore, investigate the same physical process.

4.1. Picosecond Reflectivity Measurements

Figures 2 and 3 illustrate some of the results obtained with the apparatus discussed in Fig. 1 on samples of HOPG [9]. In Fig. 2, transient reflectivity profiles at 1.06 μm versus pump laser fluence at 0.53 μm are given for different times after the peak of the heating laser pulse. Reflectivity appears to decrease with fluence at all times. In particular, at sufficiently long times ($> \approx 30$ ps) a characteristic sudden drop is observed ar a laser fluence of $\approx 140\ \text{mJ} \cdot \text{cm}^{-2}$. At this excitation level, correspondingly, postirradiation modifications of the surface first appear, indicating the onset of surface melting. By extrapolating the spot size diameters of the modified area of the sample to zero, a threshold value for surface melting of $140\ \text{mJ} \cdot \text{cm}^{-2}$ is deduced. For laser fluences below this critical value a complex behavior of the reflectivity is observed, presumably related to heating of the surface. Photoexcitation of carriers in the material by the laser pulse, which produces a reflectivity increase in the visible [10], has recently been observed experimentally [11] with higher temporal resolution and sensitivity at very low excitation. The extremely small increase in

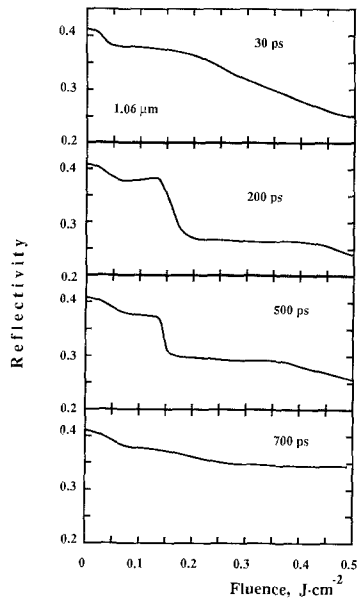

Fig. 2. Reflectivity of HOPG at 1.06 μm under 0.53-μm, 20-ps laser pulses as a function of the pump fluence ($\text{J} \cdot \text{cm}^{-2}$) for the delay times indicated.

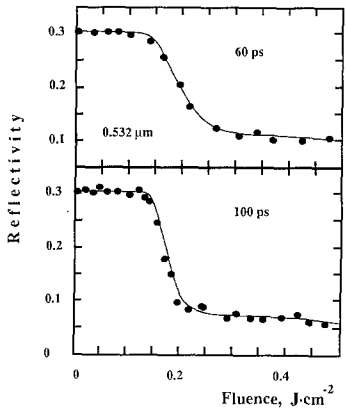

Fig. 3. Reflectivity of HOPG at 0.53 μm under 0.53-μm, 20-ps laser pulses as a function of the pump fluence ($J \cdot cm^{-2}$) for the delay times indicated.

reflectivity observed is an indirect confirmation of the relative insensitivity of the reflectivity to plasma effects in the visible region, as one should expect.

The kinetics of the liquid phase may be deduced from the reflectivity measurements at laser fluences above the critical value F_{th}. The evolution of the sharp decrease in reflectivity gives some indications of the thickness of the material being melted as well as of its optical properties.

The same considerations apply to the reflectivity curves in the visible illustrated in Fig. 3. For laser excitations below the critical value F_{th}, variations of the reflectivity after laser irradiation are not observed with the sensitivity of the experiment. As soon as the critical fluence is exceded, however, a drastic change of the reflectivity occurs, from ≈ 30 to less than 10%. These low reflectivity values occur very early after the exciting laser pulse, indicating very fast changes in the initially shallow molten depth. Similar decreases in reflectivity of liquid graphite have also been observed in the infrared (1.9 μm) and in the ultraviolet (0.266 μm). Comparable results have been obtained with natural graphite crystals.[3] Reflectivities versus photon energy for a 500 $mJ \cdot cm^{-2}$ green exciting pulse taken 100 ps after excitation are summarized in Fig. 4, where, for comparison, the initial reflectivity curve is also plotted. The curve interpolating the four data points at high temperature has a similar behavior, although a lower value than the initial one. These values are however higher than the reflectivity

[3] I am indebited to Prof. G. Scoles for providing the natural graphite crystals used in the experiments.

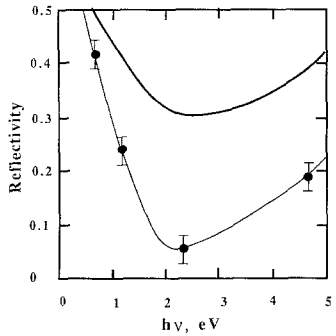

Fig. 4. Observed reflectivities versus photon energy in graphite 100 ps after excitation with 0.5 J · cm^{-2}, 0.53-μm, 20-ps laser pulses (circles). For comparison, the reflectivity of unirradiated graphite is also shown.

curves given in the literature [12] for carbon aggregates such as glassy carbon.

4.2. Picosecond Ellipsometry

From the reduced reflectivity values one can immediately deduce smaller values for both the real and the imaginary parts of the index of refraction [10]. Quantitative evaluation of these optical parameters, however, requires two measurements to be made in identical conditions. This has been done at 1.06 μm by using a time-resolved ellipsometric technique which enables the evaluation of reflectivities R_p and R_s for radiation linearly polarized in the plane of incidence and perperdicularly to it, respectively. In order to perform such measurements, however, angles of incidence different from 90° have to be used. It turned out, however, that reflectivity changes upon melting become most evident for p-polarization at large angles of incidence. In particular, Fig. 5 shows the reflectivity curves obtained at 75° incidence for s- and p-polarized beams at 1.06 μm for a delay of 200 ps between pump and probing laser pulses. While for the s-polarized radiation a small decrease in reflectivity is observed for fluences above the critical value for melting, the corresponding measurement in p-polarized light shows a sudden increase in the reflectivity of a factor ≈ 2, indicating that for the molten phase the pseudo-Brewster angles has been exceeded. Also, the occurrence of an increase in reflectivity at high temperature further supports the notion of minimal evaporation of material

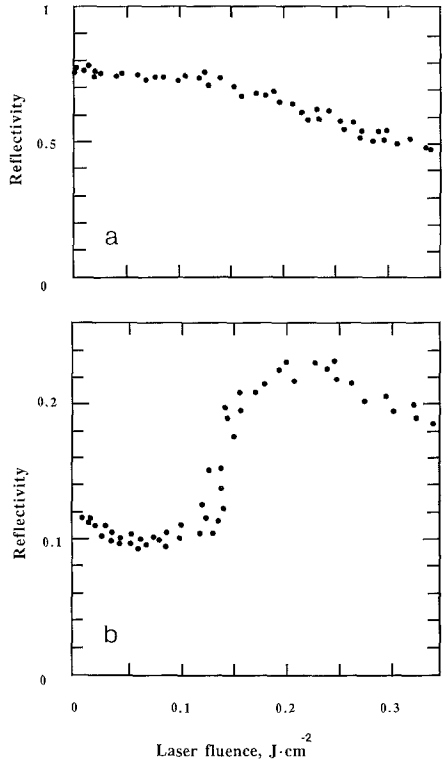

Fig. 5. Observed reflectivities of HOPG at 1.06 μm, 200 ps after irradiation by a 20-ps, 0.53-μm laser pulse, versus laser fluence. (a) s-reflectivity; (b) p-reflectivity.

from the hot surface. In other words, the observations correspond to actual changes in optical properties of the surface itself.

The results of the ellipsometric measurements performed at 1.06 μm are summarized in Figs. 6 and 7, where reflectivities versus angle of incidence have been plotted for unirradiated graphite and for samples irradiated with $\approx 250\,\mathrm{mJ \cdot cm^{-2}}$ pulses, 200 ps after the peak of the laser pulse. The best-fitting curves obtained for unperturbed graphite give an index of refraction $n_0 = 2.9 + i2.06$, in fair agreement with the data in the literature. Due to the strong anisotropy of the graphite lattice, which corresponds to a negative uniaxial absorbing crystal, p-polarization depends also on an extraordinary index of refraction, for which a value $n_e \approx 2 + i0.25$ is obtained from the measurements. The decrease in reflectivity in the high-temperature phase is documented in Fig. 7. A best

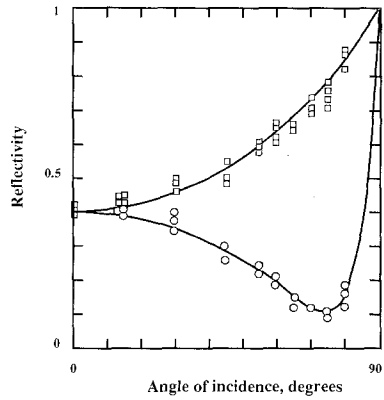

Fig. 6. s (upper branch)- and p-reflectivities at 1.06 μm for unirradiated HOPG versus angle of incidence ϑ.

fitting of all the data taken at various angles give a reduced value for the index of refraction $n \approx 1.3 + i1.2$. Similar measurements were performed in the visible at 0.53 μm, using the infared laser pulse at 1.06 μm as a pump. Scattering of the data has prevented a determination of the index of refraction for the high-tempedrature phase at this wavelength, although it has confirmed that n should fall in the region $n \approx 1 + i0.5$.

Through time-resolved ellipsometry of picosecond irradiated graphite, quantitative evaluation of the index of refraction and, therefore, of the

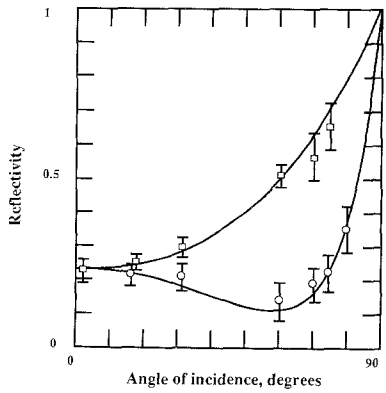

Fig. 7. s (upper branch)- and p-reflectivities at 1.06 μm for HOPG versus angle of incidence ϑ, $\approx$200 ps after irradiation with a 20-ps, 280 mJ $\cdot$ cm^{-2}, 0.53-μm laser pulse.

complex dielectric function has been carried out. A reduced index of refraction at 1.06 μm indicates a reduction in the dielectric function ε as well. However, since ε is made up by lattice and electron contributions, it is not possible to assess the relative change of each term. The observations that both real and imaginary parts of the dielectric function are reduced at high temperatures indicate that changes in the lattice contribution must occur. That this might be the only change or that also free electron contributions to the dielectric function might vary at high temperature is a question still to be answered. The behavior of the high-temperature reflectivity, as illustrated in Fig. 4, however, points toward a structure which preserves some similarities to the original one. Clearly, several measurements in a broad range of wavelengths are needed in order to extract information on the structure of the liquid phase of graphite.

5. CONCLUSIONS

The investigations of high-temperature condensed matter rely on the possibility of reaching the desired regime as well as of evaluating its relevant properties. High-power picosecond lasers seem to match both these basic requirements by providing efficient heating and noninvasive time-resolved diagnostic tools. Application of these techniques seems particularly attractive for high-melting point solids when fast evaporation of the hot material may affect the measurements. The preliminary results presented here on high-temperature graphite illustrate well the capabilities of these techniques.

ACKNOWLEDGMENT

The experiments described in this paper were performed at the Division of Applied Sciences, Harvard University, and were supported by the U.S. Office of Naval Research under Contract N00014-84-K-04654.

REFERENCES

1. N. Bloembergen, *Mat. Res. Soc. Symp. Proc.* **51**:3 (1986).
2. J. Fujimoto, Private communication.
3. J. M. Liu, R. Yen, H. Kurz, and N. Bloembergen, *Mat. Res. Soc. Symp. Proc.* **4**:23 (1982).
4. G. E. Gellison, Jr., and D. H. Lowndes, *Appl. Phys. Lett.* **48**:721 (1986).
5. P. M. Fauchet and W. L. Nigham, Jr., *Appl. Phys. Lett.* **48**:785 (1986).
6. A. G. Whittaker, P. L. Kitner, L. S. Nelson, and N. Richardson, *Aerospace Corp. Rep.* No. SD-TR-81-60 (unpublished).
7. T. Venkatesan, D. C. Jacobson, J. M. Gibson, E. S. Elman, G. Braunstein, M. S. Dresselhaus, and G. Dresselhaus, *Phys. Rev. Lett.* **53**:360 (1984).

8. J. Steinbeck, G. Braunstein, J. Speck, M. S. Dresselhaus, C. Y. Huang, A. M. Malvezzi, and N. Bloembergen, *Mat. Res. Soc. Symp. Proc.* **74**:263 (1987).
9. C. Y. Huang, A. M. Malvezzi, N. Bloembergen, and J. M. Liu, *Mat. Res. Soc. Proc.* **51**:245 (1986).
10. A. M. Malvezzi, N. Bloembergen, and C. Y. Huang, *Phys. Rev. Lett.* **57**:146 (1986).
11. J. Heremans, C. H. Olk, G. L. Eesley, J. Steinbeck, and G. Dresselhaus, *Phys. Rev. Lett.* **60**:452 (1988).
12. E. A. Taft and H. R. Philipp, *Phys. Rev.* **138**:A197 (1965).